

Electronic Properties of Si and Ge Atoms Doped In Clusters: In_nSi_m and In_nGe_m

Minoru Akutsu,[†] Kiichirou Koyasu,[†] Junko Atobe,[†] Ken Miyajima,[†] Masaaki Mitsui,[†] and Atsushi Nakajima^{*,†,‡}

Department of Chemistry, Faculty of Science and Technology, Keio University, 3-14-1, Hiyoshi, Kohoku-Ku, Yokohama 223-8522, Japan, and CREST, Japan Science and Technology Agency (JST), c/o Department of Chemistry, Keio University, Yokohama 223-8522, Japan

Received: September 11, 2006; In Final Form: November 25, 2006

Electronic properties of silicon and germanium atom doped indium clusters, In_nSi_m and In_nGe_m , were investigated by photoionization spectroscopy of the neutrals and photoelectron spectroscopy of the anions. Size dependence of ionization energy and electron affinity for In_nSi_1 and In_nGe_1 exhibit pronounced even–odd alternation at cluster sizes of $n = 10–16$, as compared to those for pure In_n clusters. This result shows that symmetry lowering with the doped atom of Si or Ge results in undegeneration of electronic states in the 1d shell formed by monovalent In atoms.

1. Introduction

The electronic and structural properties of clusters have been extensively studied over the past two decades.^{1–6} The stability of the clusters has been well-explained in terms of geometric and electronic factors. Geometric packing makes the surface energy of the cluster lower. For instance, Ar_n , Ca_n , and Ba_n exhibit magic-numbered clusters explained by the geometric stabilization of close-packing.^{2,3} On the other hand, the electronic stability of magic-numbered metal clusters has been predicted successfully by the electron shell model.⁴ This model treats only the total number of valence electrons in the cluster and has been applied mainly to homogeneous metal clusters, such as Na_n , K_n , and Al_n .^{4–6} It can be expected that clusters that satisfy both geometric and electronic factors should be very stable.

A binary cluster allows us to produce a cluster with specific stability because heterogeneous atom doping enables us to control geometric/electronic properties of clusters by an appropriate choice of the second element. In fact, the discovery of a magic cluster in binary clusters has been extensively reported experimentally and theoretically.⁷ Recently, in metal-encapsulated clusters, some magic clusters have been observed by photoelectron spectroscopy and mass spectrometry. For example, W@Au_{12} and Ti@Si_{16} have highly symmetric structures (icosahedral and Frank–Kasper-type) having 18 and 20 valence electrons, which correspond to the shell-filling number of the electron shell model.^{8,9} However, the application of the electron shell model to binary clusters is not always appropriate because the model is based on the assumption that the almost free valence electrons in the metal are subjected to a uniform potential.

Recently, a systematic study of whether the electron shell model can be applied to binary clusters has been performed on binary aluminum (Al) clusters both experimentally and theoretically.^{10–12} However, there are only a few studies concerning indium, In_n , clusters that belong to the same group as Al.^{13–15} This is probably because spectroscopic studies as

well as theoretical calculations are rather difficult to perform due to the large number of valence electrons, electronic states, and geometrical isomers. Broyer et al. have reported that the liquid-like behavior of indium clusters is stabilized by an electronic shell structure effect rather than a geometrical one.¹⁵

In this study, electronic properties of binary indium clusters were studied, in which silicon (Si) and germanium (Ge) atoms were used as a dopant in In_n clusters. Doping by the second element enables us to change the number of valence electrons. Both Si and Ge atoms have four valence electrons (s^2p^2) in contrast with one or three valence electrons in In atoms (s^2p^1). Here, we use mass spectrometry, ionization energy measurements, anion photoelectron (PE) spectroscopy, and adsorption reactivity to evaluate the stabilities and electronic properties of Si or Ge atom doped In_n clusters. The quantitative evaluation of ionization energy (E_i) and electron affinity (E_a) for In_nSi_m and In_nGe_m provides an electronic picture that symmetry lowering by a heterogeneous atom leads to undegeneration of electronic shell structures.

2. Experimental Procedures

Details of the experimental setup are described elsewhere.^{16,17} An atom of a group 14 element (Si and Ge) was doped into indium (In) clusters by double laser vaporization of a group 14 element rod and an In metal rod with He carrier gas. The neutral clusters thus formed were photoionized with an F_2 excimer laser (7.90 eV) and accelerated with a constant electric field, while the cluster anions were directly accelerated with a pulsed electric field. The accelerated clusters were mass analyzed with a time-of-flight (TOF) mass spectrometer.

The ionization energies (E_i) of the clusters were determined from the photoionization efficiency (PIE) curves measured by changing the ionization photon energy in 0.06–0.09 eV intervals over the range of 5.3–6.4 eV with an optical parametric oscillator (OPO) laser pumped by a Nd^{3+} :YAG laser.¹⁸ The fluences of the tunable UV laser and the fixed wavelength reference laser were both monitored by a pyroelectric detector and were kept at 100–200 $\mu\text{J}/\text{cm}^2$ to avoid multiphoton processes. The normalized photoionization intensity, I_{eff} , was evaluated by the ratio of the signal intensity I_{OPO} to the reference

* Corresponding author. Fax: +81-45-566-1697. E-mail: nakajima@chem.keio.ac.jp.

[†] Keio University.

[‡] Japan Science and Technology Agency.

signal intensity I_{ref} including the normalization of the laser fluencies of both ionization lasers. The reference laser was an ArF excimer laser (193 nm, 6.43 eV). The E_i values of the clusters were determined from the final decline of the PIE curves to the baseline. The fitting error was mainly due to the uncertainty in the determination of the linear increase of PIE curves and is estimated to be typically about 0.05 eV. It is noted that the obtained E_i values are ionization threshold energies and are not necessarily adiabatic ones.

The photoelectron (PE) spectra of the cluster anions were measured using a magnetic bottle TOF photoelectron spectrometer.¹⁷ The mass-selected cluster anions were photodetached with the fifth harmonic (213 nm; 5.82 eV) of the Nd³⁺:YAG laser at a 20 Hz repetition rate while the pulsed valve was synchronized to half this repetition rate (10 Hz). This alternative data acquisition for background subtraction considerably reduced the contribution of scattered electrons generated by the detachment laser irradiations. The photoelectron signal was typically accumulated to 5000–30 000 shots. The energy resolution was typically about 50 meV (full width at half-maximum) at a 1 eV electron energy. The energy of the photoelectrons was calibrated by measuring the photoelectric spectra of Au⁻. The laser power for photodetachment was in the range of 2–3 mJ/cm². Although the ionization of the dissociation product of an In atom was also observed as a competitive process with the photodetachments, the PE spectrum shape exhibited no other laser power dependence such as peak broadening and additional peak appearance.

Adsorption reactivity of the clusters was measured using a flow-tube reactor (FTR) combined with the cluster source. O₂ gas diluted by He (3% O₂ in He) gas was used as the reactant gas and was injected into the FTR. The binary cluster was synchronously mixed with the reactant gas pulse at the FTR and reacted with the reactant molecule. Mass spectra of the neutral cluster were measured before and after the reaction, and the adsorption reactivity was calculated by comparing the two mass spectra.¹⁹

3. Results and Discussion

3.1. Mass Spectra and Mass Distributions of In_nSi_m and In_nGe_m. Figure 1a,b shows typical TOF mass spectra and mass distributions of neutral In_nSi_m and In_nGe_m clusters obtained in this study. As seen in Figure 1a, the clusters of In₁₂Si₁ and In₁₂Ge₁ are produced more abundantly than the neighboring clusters. From the mass distributions shown in detail in the right side of Figure 1, the In_nSi₁ cluster with $n = 10, 12, 14,$ and 16 and the In_nSi₂ cluster with $n = 10, 12,$ and 14 are relatively more abundant than neighboring clusters. In the case of In_nGe_m neutral clusters, the In_nGe₁ clusters with $n = 10$ and 12 and the In_nGe₂ clusters with $n = 12$ are also prominent. Although In₁₂Si₁ and In₁₂Ge₁ might take on an icosahedral structure of 13 atoms, the magic-numbered behavior was less prominent when compared to aluminum binary clusters, such as aluminum–boron²⁰ and aluminum–silicon.²¹ For In_nSi_m and In_nGe_m, even–odd alternation seems to predominate in the mass distribution. In general, even numbers of total valence electrons can electronically stabilize the corresponding cluster with their pairing energy. Since an In atom has one or three valence electron(s), even-numbered In atoms, such as $n = 10, 12, 14,$ and 16 , should be more stable than odd-numbered ones. In fact, in the study of pure In_n clusters, it has been reported that the stability of the In_n cluster is governed by the electronic factor rather than the geometric one.¹⁵ To determine the electronic properties quantitatively, both photoionization and photoelectron spectroscopy were applied to the In_nSi_m and In_nGe_m clusters.

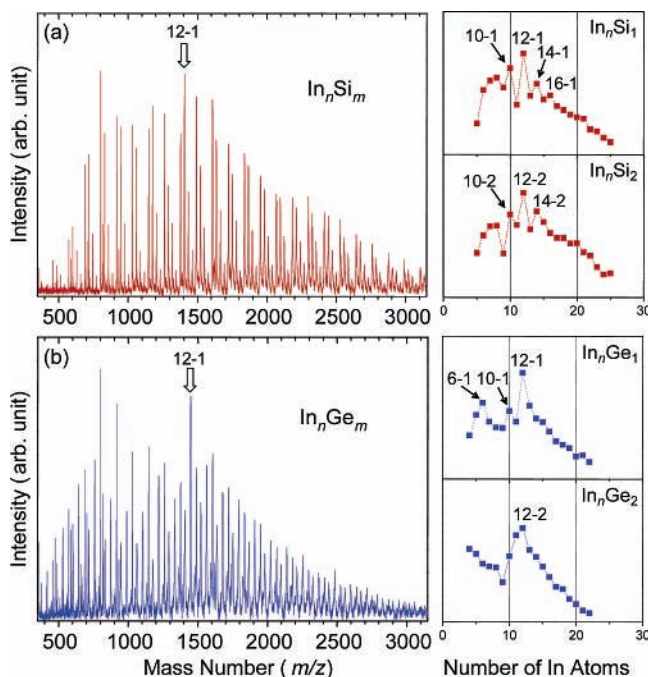


Figure 1. Time-of-flight mass spectra and mass distributions of neutral (a) In_nSi_m and (b) In_nGe_m clusters, measured with F₂ laser (7.90 eV, 157 nm)

3.2. Ionization Energy of In_n, In_nSi₁, In_nSi₂, and In_nGe₁.

The E_i values of In_nSi_m ($m = 0–2$) and In_nGe₁ were determined from their PIE curves. Figure 2 shows the E_i values of In_nSi_m ($m = 0–2$) and In_nGe₁ together with a couple of typical PIE curves. There have been several reports of the E_i values of pure In_n clusters with different production and ionization methods,^{14,22} and these E_i values are consistent with our results within experimental uncertainties.

Since the E_i value shows the energy difference between a neutral cluster and the corresponding cation, one can expect that the E_i of a stable neutral cluster is higher than that of the neighboring clusters when the neutral cluster is stable at a specific cluster size due to an electronic and/or a geometric factor(s). In Figure 2a, the E_i values of In₈ and In₁₈ are higher than the neighboring clusters, although the outstandingness of In₁₈ is much less prominent. It is known that no In_n clusters cause the s–p hybridization at least with $n \leq 15$,^{13,22} while an indium atom behaves as trivalent in the bulk. Broyer et al. have reported that the electronic structure of larger In_n clusters ($n < 200$) can be interpreted in the framework of the electron shell model of trivalent In atoms.¹⁵ Thus, it seems reasonable to regard an In atom as a monovalent atom in the small In_n clusters. Hence, the local maxima in the E_i values of In₈ and In₁₈ can be explained by the closed electronic shell structures of monovalent In atoms because the total number of valence electrons for In₈ and In₁₈ are 8 and 18, which complete the 1p and 1d shells of the electron shell model.

As seen in Figure 2b–d, even–odd oscillation in E_i values appear with the doping of Si and Ge atoms; the E_i values of In_nSi₁ and In_nGe₁ with $n = 10–16$ and In_nSi₂ with $n = 10–12$ exhibit prominent even–odd oscillation. Interestingly, the even–odd oscillation of E_i values disappears at larger sizes. The even–odd oscillation is attributed to the pairing energy, and even-numbered valence electrons in the clusters cause higher E_i as compared to odd-numbered ones. This pattern is actually quite consistent with that of the mass spectra in Figure 1, except for In₁₄Si₂: clusters having even-numbered valence electrons are rather abundant in the mass distributions.

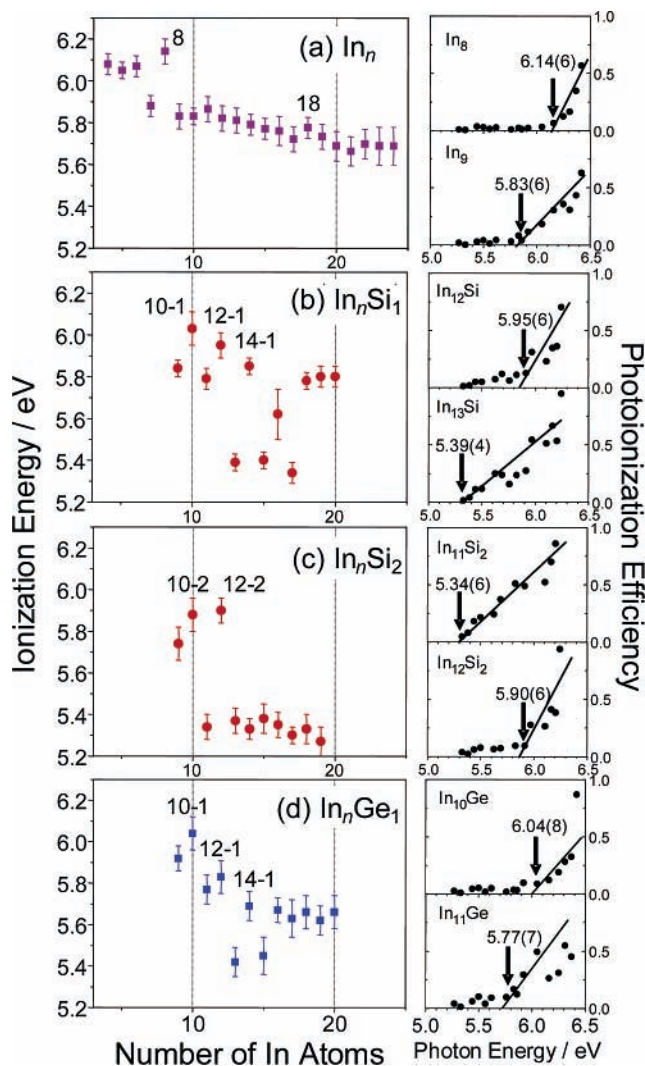


Figure 2. Ionization energies of (a) In_n ($n = 4-24$), (b) In_nSi_1 ($n = 9-20$), (c) In_nSi_2 ($n = 9-19$), and (d) In_nGe_1 ($n = 9-20$) clusters. Photoionization efficiency curves for selected clusters are shown on the right side. Down arrows indicate the ionization thresholds. Numbers in parentheses indicate experimental values in electronvolts with uncertainties: 6.14(6) represents 6.14 ± 0.06 .

Assuming monovalent In atoms and tetravalent Si/Ge atoms, valence electrons are partially filled in the 1d shell, at the sizes of $n = 9-17$ for the In_n clusters and $n = 5-13$ for the $\text{In}_n\text{Si}/\text{In}_n\text{Ge}$ clusters. The emphasized even-odd oscillation of E_i shows that the doping of Si and Ge somewhat surprisingly leads to undegeneration of electronic states in the 1d shell.

3.3. Photoelectron spectra of In_n^- , In_nSi_1^- , and In_nGe_1^- . Figure 3 shows the PE spectra at 213 nm (5.826 eV) for the cluster anions of In_n^- , In_nSi_1^- , and In_nGe_1^- with $n = 8-16$. Anion PE spectroscopy is a powerful method for direct observation of the cluster's electronic structure. For In_n^- clusters, our PE spectra at 213 nm are very consistent with those reported by others, although the detachment wavelength is different between 355 and 213 nm.¹³ Note that a sharp peak was observed around 5.5 eV in all of the spectra shown in Figure 3. Taking into account the E_i of the In atom (5.785 eV) and the energy difference (0.274 eV) between the ground state (^2P , $J = 1/2$) and the excited state (^2P , $J = 3/2$) of the In atom, we ascribe the sharp peak to the detachment from the excited state of the In atom (^2P , $J = 3/2$). Note that photoelectrons from In (^2P , $J = 1/2$) were also observed with almost the same intensity, although the second peak is not shown in the PE spectra.

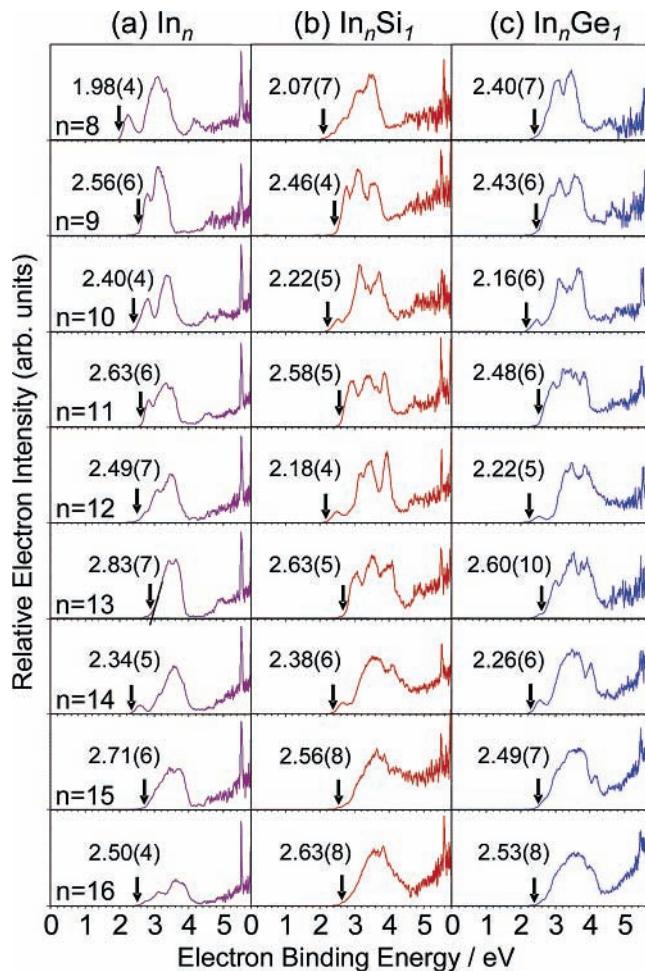


Figure 3. Photoelectron spectra of (a) In_n^- , (b) In_nSi_1^- , and (c) In_nGe_1^- clusters ($n = 8-16$) measured at photon energy of 5.83 eV (213 nm). Numbers in parentheses indicate experimental values of threshold detachment energy (electron affinity) in electronvolts with uncertainties: 1.98(4) represents 1.98 ± 0.04 .

Therefore, we can deduce that light irradiation detaches the electron of the In_n^- and also dissociates the In_n cluster into an In atom (^2P) atom and In_{n-1} .

The overall spectral features of In_nSi_1^- and In_nGe_1^- clusters are quite similar to one another for the same cluster size (n). This result implies that In_nSi_1^- and In_nGe_1^- with the same size have similar geometric and electronic structures due to the isoelectronic structures of Si and Ge atoms. In particular, the In_nX_1^- ($X = \text{Si}$ and Ge) with $n = 10, 12$, and 14 exhibit a small hump at lower electron binding energy (2.2 to ~ 2.6 eV), and detachment thresholds show even-odd oscillation. The threshold energy of detachment at even n is small and large for odd n . Considering that these clusters have a higher abundance and higher E_i than neighboring clusters, these small humps are attributed to an excess electron detachment from the SOMO of In_nX_1^- . When the neutral cluster has a closed electronic structure, an excess electron in the cluster anion should occupy the lowest unoccupied molecular orbital (LUMO), namely, a singly occupied molecular orbital (SOMO) is formed. Therefore, it is reasonable to conclude that these small peaks are attributed to the SOMO of In_nX_1^- with $n = 10, 12$, and 14 and that these neutral clusters have closed electronic structures having the HOMO-LUMO gap of about 0.8 eV. Note that in the PE spectra for In_nSi_1^- and In_nGe_1^- clusters, prominent even-odd oscillation of threshold energy (electron affinity) can be seen

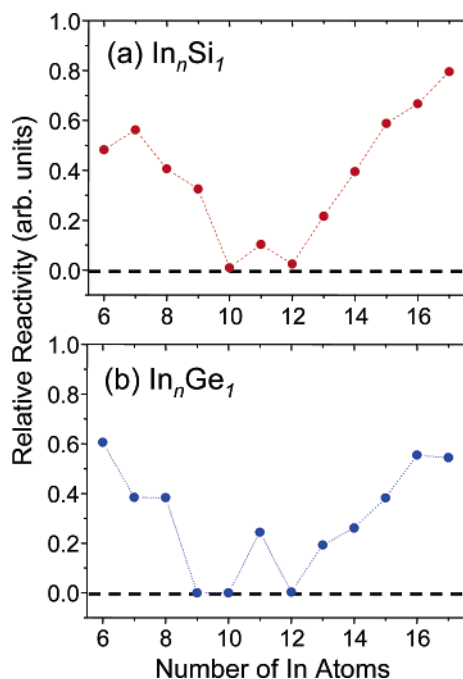


Figure 4. Adsorption reactivity of (a) In_nSi_1 and (b) In_nGe_1 with oxygen molecules.

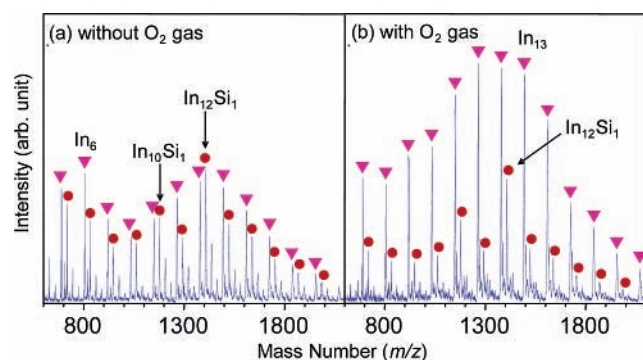


Figure 5. Mass spectra of In_nSi_1 measured (a) without O_2 gas and (b) with O_2 gas. In spectra a and b, the peaks of pure In_n clusters and In_nSi_1 binary clusters are labeled by the solid triangle (\blacktriangledown) and the solid circle (\bullet), respectively. The scale of intensities in both the mass spectra is common, and the ion intensities represent their relative abundance.

at $n = 9\text{--}14$, which is somewhat larger when compared to that of In_n^- clusters.

3.4. Adsorption Reactivity of In_nSi_1 and In_nGe_1 . The reactivity of neutral In_nSi_1 and In_nGe_1 clusters with oxygen molecules enables us to deduce the geometric and electronic structures of these clusters. As shown in Figure 4a,b, the reactivity has local minima at $n = 10$ and 12 for In_nSi_1 and at $n = 9, 10,$ and 12 for In_nGe_1 . This result indicates that In_{10}Si (In_{10}Ge) and In_{12}Si (In_{12}Ge) are electronically or geometrically stable as compared to other size clusters. Note that the increase in pure In_n cluster abundance was observed only for In_nSi_1 after reaction with O_2 as shown in Figure 5. This phenomenon suggests that a Si atom of the In_nSi_m cluster reacts with O_2 molecules and that the elimination reaction of a Si atom preferably takes place to form an In_n cluster and SiO or SiO_2 . Since the E_i values of these oxide products (SiO : 11.49 eV)²³ are higher than the photon energy of the F_2 laser (157 nm: 7.90 eV), the counterpart of SiO or SiO_2 cannot be observed in the photoionization mass spectrum.

Considering these results, the reactivity of In_nSi_1 toward O_2 molecules might provide information about the location of the

Si atom in the In_nSi_1 clusters. However, the clusters having low reactivity in Figure 4 correspond well to the clusters having higher E_i values in Figure 2. Since the reaction with O_2 is dominated by electron transfer from a cluster to O_2 rather than by geometric factors,¹⁴ it reasonably seems that the reactivity is determined by the magnitude of ionization energy. Although it is theoretically and experimentally revealed that $\text{Al}_{12}\text{Si}_1$ clusters have I_h symmetric structures, in which a Si atom is surrounded by Al atoms,^{21,24} it was very hard to deduce whether $\text{In}_{12}\text{Si}_1$ has the cage structure where a Si atom is encapsulated by In atoms, by using the adsorption reactivity.

3.5. Electronic Structures of In_nSi_m and In_nGe_m . As suggested by the mass distributions, the quantitative evaluation of electronic properties and adsorption reactivity reveal that In_nX_1 with $n = 10, 12,$ and 14 and In_nX_2 with $n = 10$ and 12 ($\text{X} = \text{Si}$ and Ge) exhibit partially or fully closed electronic structures. For indium, it is known that the In clusters satisfy an electronic shell structure, where In atoms behave as monovalent atoms at $n \leq 15$ ¹³ and the critical size at which the valence of an In atom in In_n becomes trivalent has not been established. The important information to estimate the changing size from monovalent to trivalent is the $s \rightarrow p$ excitation energy. Group 3 elements are characterized by the s^2p^1 configuration yielding 2P atomic ground states. The s orbital binding energies increase as nuclear charge increases, resulting in higher $s \rightarrow p$ excitation energies for indium (In: 4.3 eV) as compared to aluminum (3.6 eV).²⁵ Consequently, an Al atom in Al_n clusters causes the $s\text{--}p$ hybridization and has a trivalent character above $n = 9$,²⁶ while an In atom in In_n clusters with $n \leq 15$ has a monovalent character.^{13,22} The doping of a Si or Ge atom to In_n clusters might make the $s \rightarrow p$ excitation energies smaller and the valence of an In atom in In_n clusters trivalent because of the change of geometric and electronic structure of an In_n cluster by heterogeneous atom doping (e.g., cage structure). In fact, it has been reported that the trivalent character of In atoms is emphasized when an oxygen (O) atom is doped into In clusters.²⁷ Although theoretical calculations are needed, the size dependence of the E_i and E_a measured in this study do not show obvious evidence of $s\text{--}p$ hybridization: the E_i of $\text{In}_{12}\text{Si}/\text{In}_{12}\text{Ge}$ is not low, but it does not take a maximum as compared to its neighbors. The E_a of $\text{In}_{12}\text{Si}/\text{In}_{12}\text{Ge}$ is not high, but it does not take a minimum as compared to its neighbors. Hence, it is reasonable to conclude that an In atom in In_nSi_1 and In_nGe_1 ($n \leq 20$) in this study behaves as a monovalent atom.

Assuming that Si and Ge atoms are tetravalent, In_nSi and In_nGe at $n = 10\text{--}14$ take an electronic structure having a partially or fully filled $1d$ shell. Mixing a heterogeneous atom in a homogeneous cluster usually causes the symmetric lowering of geometric structure. Consequently, the even–odd alternations of E_i and E_a are attributed to the undegeneration of electronic states in the $1d$ shell. Although trivalency in In atoms may allow In_{10}Si (In_{10}Ge) and In_{12}Si (In_{12}Ge) to complete $1f$ shell and $2p$ shells, as discussed previously, the experimental data show no explicit evidence that the valence of an In atoms changes from monovalent to trivalent.

4. Conclusion

We produced group 14 element atom doped indium clusters in the gas phase and examined their electronic properties by using mass spectrometry, E_i measurements, anion PE spectroscopy, and adsorption reactivity. Size dependence of E_i and E_a for In_nSi_1 and In_nGe_1 exhibit pronounced even–odd alternation at cluster sizes of $n = 10\text{--}16$, which is considerably greater as compared to those for pure In_n clusters. This result shows that

symmetry lowering with the dopant (Si or Ge) results in the undegeneration of the 1d shell caused by monovalent In atoms, and that an In atom in In_nSi_l and In_nGe_l ($n \leq 20$) in this study behaves as a monovalent atom.

Acknowledgment. This work is partly supported by the Ministry of Education, Culture, Sports, Science, and Technology, Grant-in-Aid for the 21st Century COE Keio LCC. K.K. is grateful to a Research Fellowship of JSPS for Young Scientists.

References and Notes

- (1) de Heer, W. A. *Rev. Mod. Phys.* **1993**, *65*, 611.
- (2) Echt, O.; Sattler, K.; Recknagel, E. *Phys. Rev. Lett.* **1981**, *47*, 1121.
- (3) Rayane, D.; Melinon, P.; Cabaud, B.; Hoareau, A.; Tribollet, B.; Broyer, M. *Phys. Rev. A* **1989**, *39*, 6056.
- (4) Knight, W. D.; Clemenger, K.; de Heer, W. A.; Saunders, W. A.; Chou, M. Y.; Cohen, M. L. *Phys. Rev. Lett.* **1984**, *52*, 2141.
- (5) Saunders, W. A.; Clemenger, K.; de Heer, W. A.; Knight, W. D. *Phys. Rev. B* **1985**, *32*, 1366.
- (6) Persson, J. L.; Whetten, R. L.; Cheng, H. P.; Berry, R. S. *Chem. Phys. Lett.* **1991**, *186*, 215.
- (7) Janssens, E.; Neukermans, S.; Lievens, P. *Curr. Opin. Solid State Mater. Sci.* **2004**, *8*, 185.
- (8) Li, X.; Kiran, B.; Li, J.; Zhai, H. J.; Wang, L. S. *Angew. Chem., Int. Ed.* **2002**, *41*, 4786.
- (9) Koyasu, K.; Akutsu, M.; Mitsui, M.; Nakajima, A. *J. Am. Chem. Soc.* **2005**, *127*, 4998.
- (10) Li, X.; Wang, L. S. *Phys. Rev. B* **2002**, *65*, 153404.
- (11) Kawamata, H.; Negishi, Y.; Nakajima, A.; Kaya, K. *Chem. Phys. Lett.* **2001**, *337*, 255.
- (12) Bergeron, D. E.; Castleman, A. W., Jr.; Jones, N. O.; Khanna, S. N. *Chem. Phys. Lett.* **2005**, *415*, 230.
- (13) Gausa, M.; Ganteför, G.; Lutz, H. O.; Meiwes-Broer, K. H. *Int. J. Mass. Spectrom. Ion Processes* **1990**, *102*, 227.
- (14) Nakajima, A.; Hoshino, K.; Sugioka, T.; Naganuma, T.; Taguwa, T.; Yamada, Y.; Watanabe, K.; Kaya, K. *J. Phys. Chem.* **1993**, *97*, 86.
- (15) Baguenard, B.; Pellarin, M.; Bordas, C.; Lermé, J.; Vialle, J. L.; Broyer, M. *Chem. Phys. Lett.* **1993**, *205*, 13.
- (16) Nakajima, A.; Kaya, K. *J. Phys. Chem. A* **2000**, *104*, 176.
- (17) Nakajima, A.; Taguwa, T.; Hoshino, K.; Sugioka, T.; Naganuma, T.; Ono, F.; Watanabe, K.; Nakao, K.; Konishi, Y.; Kishi, R.; Kaya, K. *Chem. Phys. Lett.* **1993**, *214*, 22.
- (18) Miyajima, K.; Muraoka, K.; Hashimoto, M.; Yasuike, T.; Yabushita, S.; Nakajima, A.; Kaya, K. *J. Phys. Chem. A* **2002**, *106*, 10777.
- (19) Morse, M. D.; Gausic, M. E.; Heath, J. R.; Smalley, R. E. *J. Chem. Phys.* **1985**, *83*, 2293.
- (20) Nakajima, A.; Kishi, T.; Sugioka, T.; Kaya, K. *Chem. Phys. Lett.* **1991**, *187*, 239.
- (21) Akutsu, M.; Koyasu, K.; Atobe, J.; Hosoya, N.; Miyajima, K.; Mitsui, M.; Nakajima, A. *J. Phys. Chem. A* **2006**, *110*, 12073.
- (22) Rayane, D.; Melinon, P.; Cabaud, B.; Hoareau, A.; Tribollet, B.; Broyer, M. *J. Chem. Phys.* **1989**, *90*, 3295.
- (23) Hildenbrand, D. L.; Murad, E. *J. Chem. Phys.* **1969**, *51*, 807.
- (24) (a) Gong, X. G.; *Phys. Rev. B* **1997**, *56*, 1091. (b) Kumar, V.; Sundararajan, V. *Phys. Rev. B* **1998**, *57*, 4939. (c) Ashman, C.; Khanna, S. N.; Liu, F.; Jena, P.; Kaplan, T.; Mostoller, M. *Phys. Rev. B* **1997**, *55*, 15868. (d) Charkin, O. P.; Charkin, D. O.; Klimenko, N. M.; Mebel, A. M. *Chem. Phys. Lett.* **2002**, *365*, 494.
- (25) Moore, C. E. *Natl. Bur. Stand., Ref. Data Ser.* **1971**, 35.
- (26) Li, X.; Wu, H.; Wang, X. B.; Wang, L. S. *Phys. Rev. Lett.* **1998**, *81*, 1909.
- (27) Janssens, E.; Neukermans, S.; Vanhoulte, F.; Silverans, R. E.; Lievens, P.; Navarero-Vazquez, A.; Schleyer, P. v. R. *J. Chem. Phys.* **2003**, *118*, 5862.